The RNA-binding protein ELAVL1/HuR is essential for mouse spermatogenesis, acting both at meiotic and postmeiotic stages

Mai Nguyen Chi[a], Jacques Auriol[a], Bernard Jégou[b], Dimitris L. Kontoyiannis[c], James M.A. Turner[d], Dirk G. de Rooij[e], and Dominique Morello[a]

[a]CBD, UMR5547, IFR 109, Université Paul Sabatier, 31062 Toulouse Cedex, France; [b]INSERM U625, GERHM, Institut Fédératif de Recherche 140, F-35042 Rennes, France; [c]Institute of Immunology, Biomedical Sciences Research Center Alexander Fleming, 16672 Vari, Greece; [d]Division of Stem Cell Biology and Developmental Genetics, Medical Research Council, National Institute for Medical Research, London NW7 1AA, UK; [e]Department of Endocrinology and Metabolism, Faculty of Science, Utrecht University, 3584 CH Utrecht, The Netherlands

ABSTRACT Posttranscriptional mechanisms are crucial to regulate spermatogenesis. Accurate protein synthesis during germ cell development relies on RNA binding proteins that control the storage, stability, and translation of mRNAs in a tightly and temporally regulated manner. Here, we focused on the RNA binding protein Embryonic Lethal Abnormal Vision (ELAV) L1/Human antigen R (HuR) known to be a key regulator of posttranscriptional regulation in somatic cells but the function of which during gametogenesis has never been investigated. In this study, we have used conditional loss- and gain-of-function approaches to address this issue in mice. We show that targeted deletion of HuR specifically in germ cells leads to male but not female sterility. Mutant males are azoospermic because of the extensive death of spermatocytes at meiotic divisions and failure of spermatid elongation. The latter defect is also observed upon HuR overexpression. To elucidate further the molecular mechanisms underlying spermatogenesis defects in HuR-deleted and -overexpressing testes, we undertook a target gene approach and discovered that heat shock protein (HSP)A2/HSP70-2, a crucial regulator of spermatogenesis, was down-regulated in both situations. HuR specifically binds *hspa2* mRNA and controls its expression at the translational level in germ cells. Our study provides the first genetic evidence of HuR involvement during spermatogenesis and reveals *Hspa2* as a target for HuR.

INTRODUCTION

Spermatogenesis is a highly regulated and complex process through which spermatozoa are produced. It involves the differentiation of diploid spermatogonia into spermatocytes and then, through two successive divisions, into haploid round spermatids. Subsequently, dramatic morphological changes take place in those postmeiotic haploid germ cells that undergo an elongation phase during spermiogenesis, transforming them into mature spermatozoa. In particular, the chromatin progressively compacts while the spermatid differentiates, leading to transcriptional silencing before differentiation is completed (Kimmins and Sassone-Corsi, 2005). Thus the synthesis of proteins required for spermatozoa assembly and function is thought to rely on the appropriate storage and translational control of mRNAs that have been transcribed at earlier meiotic or postmeiotic steps (Steger, 1999, 2001). This hypothesis is strengthened by a study showing that many mRNAs that are silent during early steps of differentiation are stored in ribonucleoproteins (RNPs) and later on shift into polysomes where they are actively translated (Iguchi et al., 2006). The factors controlling mRNA fate during spermiogenesis are beginning to be identified and include RNA-binding proteins (RBPs)

that specifically control stabilization and translation of their target mRNAs. Numerous RBPs are synthesized solely in late phases of spermatogenesis, ensuring a temporal regulation of their target mRNAs (Iguchi et al., 2006). RBPs such as Miwi, Ddx25, Msy2, Sam68, and CUGBP1, have been shown to play crucial roles in spermatid differentiation as their knockout (KO) led to spermiogenic arrest and subsequent male sterility (Deng and Lin, 2002; Tsai-Morris et al., 2004; Yang et al., 2005; Kress et al., 2007).

To gain further insight into the contribution of posttranscriptional control during spermatogenesis, we focused on Embryonic Lethal Abnormal Vision (ELAV) L1/Human antigen R (HuR), an RBP that belongs to the ELAV family of proteins (Ma et al., 1996; Myer et al., 1997). HuR was first identified in somatic cells for its ability to bind an AU-rich element (ARE) contained in the 3′ UTR of c-fos and Il3 mRNAs and then to increase the stability of many ARE-containing mRNAs (reviewed in (Bevilacqua et al., 2003). RNA-immunoprecipitation (IP) assays in human colorectal carcinomas revealed that, in addition, HuR could bind mRNAs containing a U-rich 17- to 20-nucleotide-long motif, most frequently located in their 3′ UTR (Lopez de Silanes et al., 2004). Besides its protective role against mRNA degradation, HuR was also shown to regulate the translation of various mRNAs (reviewed in Galban et al., 2008).

Studies of HuR function in vivo have been compromised by the fact that its constitutive inactivation is lethal to embryos (Katsanou et al., 2009). Thus most of our knowledge comes from transformed cells or experimental situations in which the level of HuR is naturally (cancer cells) or artificially increased through the use of transgenic mice. In this respect, we previously have reported that HuR overexpression in macrophages leads to translational silencing of specific cytokine mRNAs (Katsanou et al., 2005) and that fertility is compromised in the HuR-overexpressing transgenic testis (Levadoux-Martin et al., 2003). Our recent data indicate that during normal spermatogenesis HuR expression is tightly regulated both spatially and temporally (Nguyen Chi et al., 2009). In particular, we have shown that HuR is a component of the mammalian germ cell nuage, also called the chromatoid body (CB; Parvinen, 2005). This germ cell–specific perinuclear cytoplasmic structure contains polyadenylated mRNAs and various components of microRNA and RNA-processing pathways and is therefore proposed to act as a center of mRNA storage and processing (Kotaja et al., 2006). Whereas HuR concentrates within the CB of early spermatids, it subsequently transits to polysomes together with its target ARE-containing mRNAs, suggesting that HuR participates in the control of mRNA storage/translation in spermatids (Nguyen Chi et al., 2009).

We now have studied the role of HuR during spermatogenesis by using both conditional KO and HuR-overexpressing mice. We show that inactivation of HuR in primordial germ cells (PGCs) is incompatible with proper postmeiotic cell formation and spermatid maturation. In addition, HuR overexpression in round spermatids delays spermatid differentiation and therefore the production of fully competent transgenic spermatozoa. Further analysis based on a candidate gene approach revealed that HSPA2, a protein that belongs to the 70-kDa heat shock protein (HSP70) family that is essential for male germ cell differentiation, is misregulated both in HuR-overexpressing and -deficient germ cells. Our study demonstrates that HuR is required both in meiotic and postmeiotic steps in mouse spermatogenesis and points to HSPA2 as a prominent molecular target of HuR.

RESULTS
HuR is essential for normal male fertility
To explore the biological function of HuR during spermatogenesis, we first analyzed the consequences of its inactivation in germ cells.

In view of the embryonic lethality of $Elavl1^{-/-}$ embryos (Ghosh et al., 2009; Katsanou et al., 2009), we used a conditionally defective HuR allele containing target sites for the Cre/loxP recombination system ($Elavl1$ floxed allele or $Elavl1^{fl}$; Katsanou et al., 2009) and a battery of Cre-expressing transgenic mice, including Sycp1-Cre (Vidal et al., 1998), Vasa-Cre (Gallardo et al., 2007), Vav-Cre (de Boer et al., 2003), and Nestin-Cre (http://jaxmice.jax.org/strain/002858.html), which have been shown to function exclusively (the first two) or less specifically in reproductive tissues. Except for the Vasa-Cre mice (see later in the text), the efficiency of recombination was too low to permit a complete deletion of $Elavl1$ in all germ cells. Indeed, the germ cells develop as a syncytium where cells stay connected to one another by intracellular bridges after cell division, allowing communication between cells. If recombination is not complete in one or a few of a clone, HuR expression will occur in adjacent haploid HuR^- cells, compromising further study on the consequence of HuR deletion. The passing through of the HuR protein from $Elavl1^+$ to $Elavl1^-$ haploid daughter cells was well illustrated by immunofluorescence analysis of $Elavl1^{+/-}$ testis showing that all round spermatids expressed HuR, whereas only 50% were expected to do so (Supplemental Figure S1 $Elavl1^{+/-}$ testis). The same result was obtained when analyzing $Elavl1^{fl/-}$; Sycp1-Cre testes, showing that the recombinase was not fully efficient (Supplemental Figure S1). Its inefficiency was further confirmed by crossing $Elavl1^{fl/-}$; Sycp1-Cre males with wild-type (WT) females. Approximately 50% of the pups were $Elavl1^{+/-}$ and 50% were $Elavl1^{fl/+}$, a proportion significantly different from the 100% $Elavl1^{+/-}$ expected if the Cre recombinase were fully efficient (see Supplemental Figure S1 for details).

In Vasa-Cre mice, the Cre recombinase is active in PGCs (Gallardo et al., 2007) and therefore guarantees the deletion of $Elavl1$ in the germ cells that all derive from these precursor cells (Figure 1A). To inactivate HuR specifically in PGC (genotyped as Vasa-Cre; $Elavl1^{fl/-}$), we first crossed $Elavl1^{+/-}$ mice with Vasa-Cre heterozygous mice, then selected $Elavl1^{+/-}$; Vasa-Cre males that were crossed with $Elavl1^{fl/fl}$ females (Figure 1A). Surprisingly, the number of Vasa-Cre; $Elavl1^{fl/-}$ pups was dramatically low as only four of 400 mice with such a genotype were obtained. Similarly, the transmission of the Vasa-Cre allele was lower than expected (26% instead of 50%, n = 400), whereas its transmission was at the expected Mendelian frequency in the previous (Vasa-Cre × $Elavl1^{+/-}$) generation (48%, n = 43). These results strongly suggest that, in some cases, Vasa regulatory sequences are active in early embryogenesis, leading to Vasa-Cre; $Elavl1^{-/-}$ embryos. As we previously reported, $Elavl1^{-/-}$ embryos die in utero because HuR is required for placental branching morphogenesis (Katsanou et al., 2009). Hence, midgestational embryo death led to reduced transmission of both Vasa-Cre transgene and $Elavl1^-$ allele.

Among the four PGC-specific HuR-KO animals, we obtained one female and three males. To examine male fertility, two Vasa-Cre; $Elavl1^{fl/-}$ males were crossed with untreated or superovulated WT females. Despite repeated matings, from 6 to 9 wk, no pregnant females were obtained, whereas control males ($Elavl1^{fl/fl}$, both $Elavl1$ alleles active or $Elavl1^{fl/-}$ or $Elavl1^{+/-}$, a single allele active) were fully fertile (unpublished data), strongly suggesting that Vasa-Cre; $Elavl1^{fl/-}$ males were sterile. To confirm this hypothesis, these two males were killed at 9 wk. Their testes and epididymides were remarkably smaller than those of controls, and the ratio testis/body weight was significantly different from that of control (WT or $Elavl1^{fl/-}$) males (Figure 1B and unpublished data). Immunohistochemistry (IHC) using anti-HuR antibody on HuR mutant testis sections showed the absence of HuR protein in all types of germ cells, in contrast to control ($Elavl1^{fl/-}$, $Elavl1^{fl/fl}$, or WT) testis sections
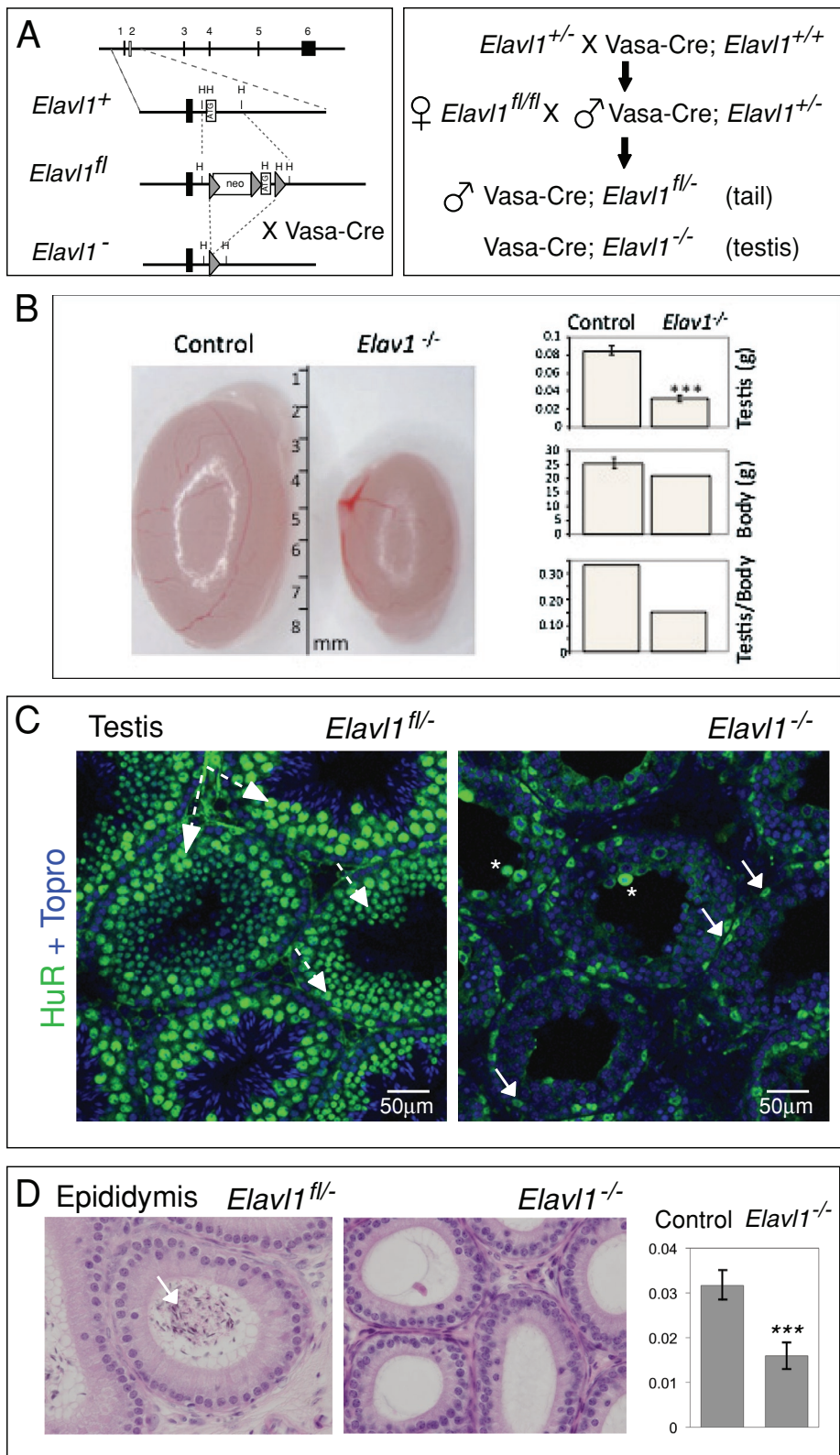
FIGURE 1: HuR KO males are sterile. (A) Left, schematic of the complete exon–intron orientation of the *HuR* locus and magnification of the region containing the ATG-containing exon 2 (gray box). In the targeted locus (*Elavl1*^{fl}), exon 2 is flanked by two loxP sites, allowing exon 2 excision by the Cre recombinase (Katsanou et al., 2009). Right, crossing strategy to target *HuR* gene deletion specifically in the germ cells. Using Vasa-cre mice expressing the Cre recombinase in the PGCs, germ cells of Vasa-Cre; *Elavl1*^{fl/–} males do not express HuR (*Elavl1*^{–/–} testis), whereas somatic tissues do (*Elavl1*^{fl/–} tail). (B) The size and weight of 9-wk-old HuR mutant testes (n = 4) were significantly reduced compared with control (*Elavl1*^{fl/+} or *Elavl1*^{fl/–}) testes (n = 8) even though

(Figure 1C for *Elavl1*^{fl/–}, Supplemental Figure S1, and unpublished data). The only positive HuR cells corresponded to the somatic Sertoli cells in which the Cre recombinase was not active. Comparative histological analysis of sectioned epididymides from WT, *Elavl1*^{+/–}, and *Elavl1*^{–/–} mutant mice revealed a complete loss of spermatozoa in mutant epididymides (Figure 1D).

Interestingly, the Vasa-Cre; *Elavl1*^{fl/–} female we obtained showed no overt ovarian abnormalities (unpublished data); its fecundity was comparable to that of control (*Elavl1*^{fl/–}) females, and deliveries were still observed at the age of 12 mo (unpublished data). In addition, upon successive mating with WT males, none of the progeny carried an *Elavl1*^{fl} allele but were all heterozygous (+/–). Even though only one Vasa-Cre; *Elavl1*^{fl/–} female was obtained, these results clearly show that the *Elavl1*^{fl} allele has efficiently been recombined in each oocyte. Thus HuR depletion in PGCs induces male sterility but does not seem to compromise female fertility.

HuR is required for the first meiotic division progression

The loss of spermatozoa in HuR-KO males suggests that germ cell differentiation is impaired. Thus we performed histological analysis of testis sections from both juvenile and adult control or mutant mice. Whereas adult testes from WT mice at 9 wk of age showed spermatogenic cells in all of the different stages of differentiation (spermatogonia, spermatocytes, round and elongated spermatids; see Figure 2, A, C, and G, for

---

HuR^{fl/–}; Vasa-Cre males were slightly lighter than their control (*Elavl1*^{fl/+} or *Elavl1*^{fl/–}) brothers. (C) Immunoconfocal analysis of HuR expression in control (*Elavl1*^{fl/–}) and mutant (*Elavl1*^{fl/–}; Vasa-Cre) tubule sections. Whereas HuR (green) is expressed in spermatocytes and all round spermatids of control *Elavl1*^{+/–} testis (dashed and solid arrows in the left panel, respectively), its expression is restricted to interstitial cells and to Sertoli cells in mutant tubules (arrow in the right panel). * indicates unspecific labeling of dead cells. All nuclei are labeled with Topro (blue). Scale bars, 50 μm. (D) Histological analysis of control (*Elavl1*^{fl/–}) and mutant (*Elavl1*^{fl/–}; Vasa-Cre) epididymides. H&E-stained sections from 9-wk-old males. Whereas control epididymis tubules contain many spermatozoa (arrow), no sperm was observed in the mutant ones. The weight (g) of mutant epididymides (n = 4) is significantly different from that of control (*Elavl1*^{fl/+} or *Elavl1*^{fl/–}) epididymides (n = 8).
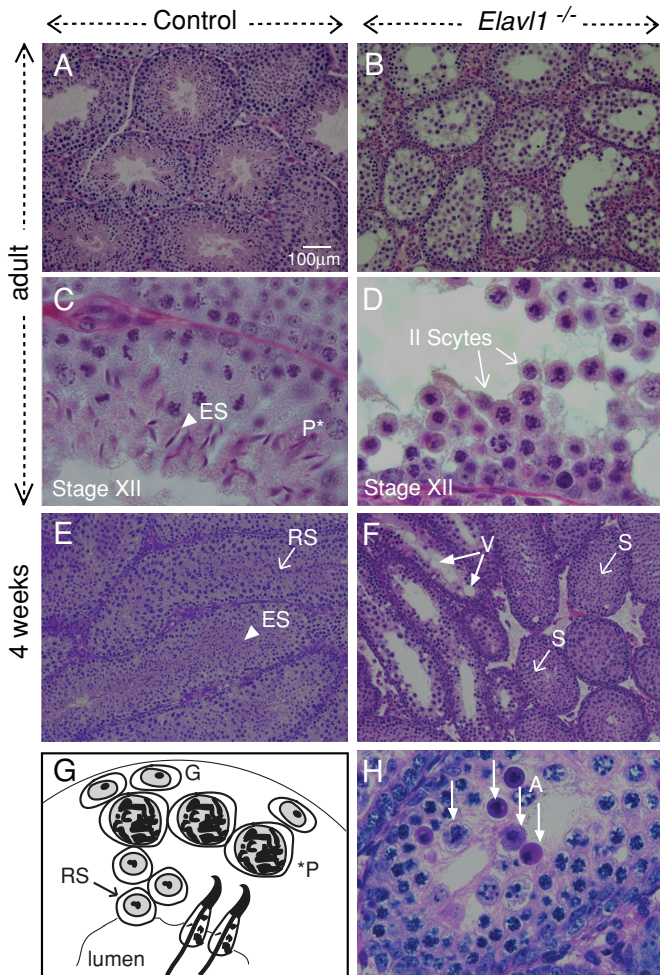
FIGURE 2: Meiotic divisions are compromised in *Elavl1⁻/⁻* testis. (A–D) Histological analysis of testis from 9-wk-old control (*Elavl1^{fl/+}*; Vasa-cre) (A and C) and mutant (*Elavl1^{fl/−}*; Vasa-cre) (B and D) mice. Sections were stained with H&E. The low-magnification views of control (A) and mutant (B) seminiferous tubules show that mutant tubules contain fewer germ cells and numerous vacuoles. Whereas control tubules contain all types of differentiating germ cells (A and C), as schematized in G, in mutant ones, germ cells differentiate normally until spermatocyte stage but apparently cannot carry out meiotic divisions (B and D). The metaphase plates of the HuR-deficient spermatocytes are irregular, the chromosomes look thick, and the cytoplasm is starting to stain, indicating apoptosis (D). Dashed arrows indicate two secondary spermatocytes (II Scytes). P, pachytene spermatocytes; ES, elongated spermatids. Twelve stages of spermatogenesis have been determined in mouse spermatogenesis on the basis of specific cell associations and key morphological criteria (Kotaja et al., 2004) that were used to stage the different sections of seminiferous tubules shown in this study. (E, F, and H) Histological analysis of testis from 4-wk-old control (*Elavl1^{fl/+}*; Vasa-cre) (E) and mutant (*Elavl1^{fl/−}*; Vasa-cre) (F and H) mice. Whereas control tubules (E) contain round (RS) and elongated spermatids (ES), spermatid formation and differentiation are compromised in mutant tubules (F and H). Approximately 50% of mutant tubules contain numerous vacuoles (V), and germ cell differentiation is arrested before postmeiotic stages (F). In a few apparently normal mutant tubules, round spermatids have begun elongation (S), but the process is delayed. The tubule shown in H shows massive cell death among the spermatocytes in meiotic divisions (A, arrows). (A, B, E, and F: ×20; C, D, and H: ×60).

their respective localization in a schematic tubule section), dramatic spermatogenic defects were observed in the testes of the two adult mutant males (Figure 2, B and D, and Supplemental Figure S1). Numerous vacuoles were observed in seminiferous tubules that contained essentially spermatocytes but lacked spermatids (Figure 2, D vs. C). Spermatocytes progressed until meiotic divisions, but meiotic divisions were compromised, and massive cell death was visible in stage XII tubules where meiotic divisions normally take place (Figure 2, B and D). At 4 wk of age, in the WT testes, all tubule cross-sections showed at least round spermatids and, in many tubules, elongating spermatids were already present as the most advanced type of germ cells (Figure 2E). By contrast, in the third remaining HuR-KO male that was killed at P29, approximately half of the tubules contained numerous vacuoles and showed a nearly complete block of spermatogenic maturation at the spermatocyte stage (Figure 2F) and numerous dead or dying cells (Figure 2H), akin to what was observed in mutant adult testes. The remaining tubules contained spermatids, as expected, but their differentiation was delayed (see later in the text; Figure 2F).

All together, these results suggest that HuR is initially required for meiotic progression. To further characterize the stage of defect in HuR mutant testes, we first thoroughly analyzed the kinetics of HuR expression during meiosis of WT males. To substage meiosis, we carried out dual immunocytochemical staining of surface-spread germ cells or testis sections using anti-HuR antibody together with anti-SYCP3, which marks a lateral component of the synaptonemal complex (Lammers et al., 1994), the dynamics of which during meiosis has been well characterized (Turner et al., 2001), or anti-phospho-H2AX histone (γH2AX) antibody that marks sites of double-strand breaks (Mahadevaiah et al., 2001). HuR was not expressed in early prophase spermatocytes (leptotene-zygotene), but accumulated as the pachytene stage progressed (Figure 3A and unpublished data). Although present in diplotene spermatocytes, HuR staining disappeared during the diplotene-metaphase I transition (Figure 3B). In postmeiotic haploid cells, HuR accumulated in round spermatids but was absent in elongated spermatids (Figure 3B and Nguyen Chi et al., 2009).

To know more precisely at which stage HuR absence could affect meiosis in HuR mutant germ cells, we then analyzed meiosis progression in mutant testes by using the combination of anti–phospho-H2AX and anti-SYCP3 antibodies. Early spermatocyte differentiation was not affected in mutant, as cells at leptotene and zygotene stages were present in normal number (Figure 3C). This result is not surprising because these cells normally do not express HuR (Figure 3A, WT). Later on during differentiation, we observed all the prophase stages from pachytene spermatocytes to the diakinesis step. Neither synapsis of homologous chromosomes nor sex body formation was perturbed (Figure 3D and unpublished data). Compared with control germ cells, however, the relative number of midpachytene spermatocytes was increased twofold whereas that of cells at diplotene and diakinesis stages was dramatically diminished (Figure 3E). This finding shows that HuR-deficient cells progress efficiently to midpachytene stage and suggests that cell death takes place just before or during meiotic divisions, leading to a strong deficit in haploid cells as shown earlier in this article (Figure 2). Collectively, our results indicate that HuR is dynamically expressed during meiosis and is required for meiotic progression.

HuR is required for spermatid differentiation

Besides tubules in which spermatogenesis was arrested, juvenile HuR-deficient testes contained ~50% of tubules in which spermatocytes
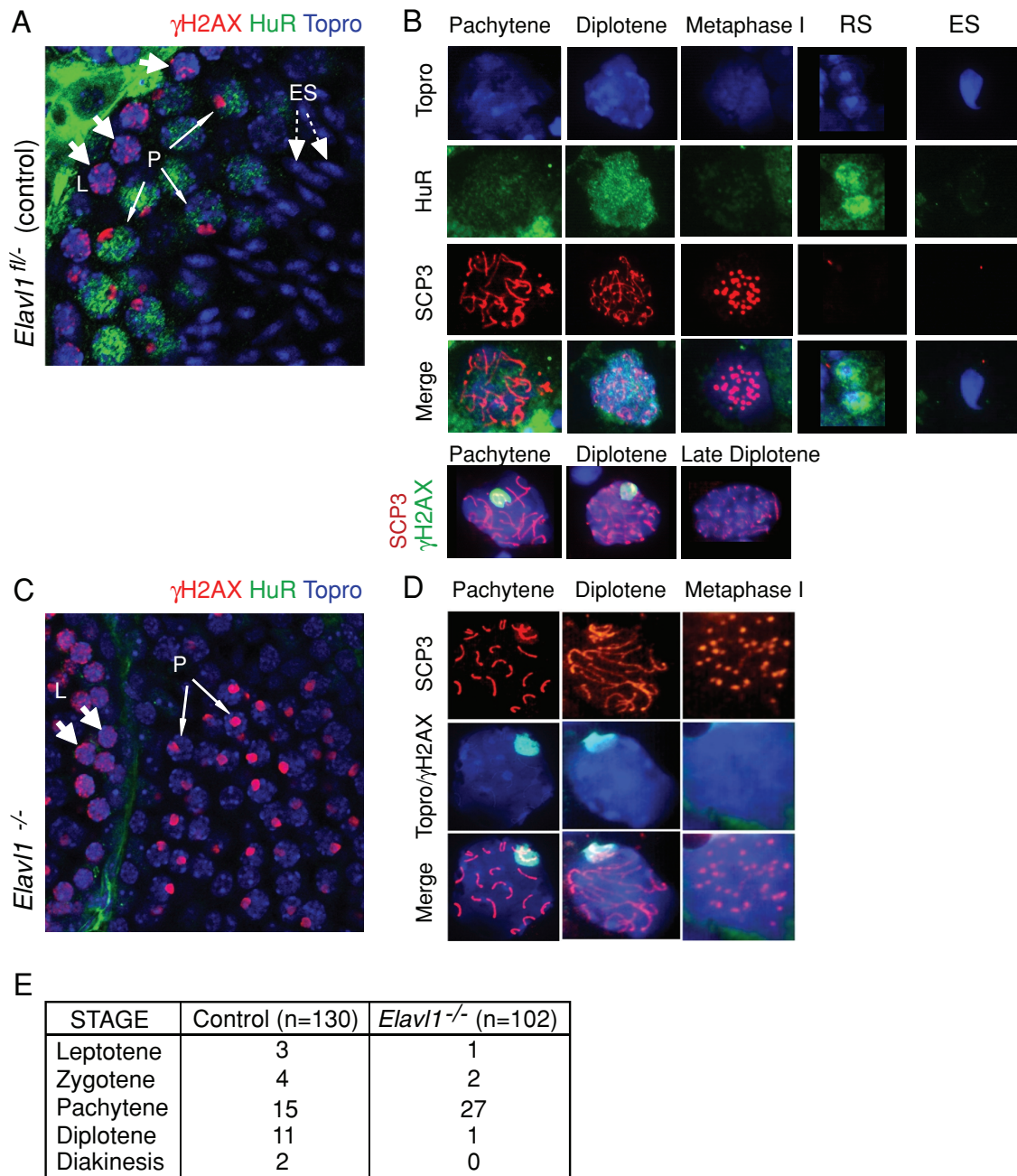
FIGURE 3: HuR expression in meiotic and postmeiotic stages. (A and C) Sections from adult (9-wk-old) control (*Elavl1*^{fl/−})
(A) or mutant (*Elavl1*^{fl/−}; Vasa-cre) (C) testis were immunostained with anti-HuR (green) and anti-γH2AX (red) and
analyzed under a confocal microscope. Neither leptotene spermatocytes (L, large arrows) nor elongated spermatids
(S, dashed arrows) express HuR, whereas pachytene spermatocytes (P, thin arrows) do express HuR in the control testis.
γH2AX-stained sex bodies are normally observed in mutant pachytene spermatocytes (C). All nuclei are labeled with
Topro. (B, D, and E) Expression of HuR during germ cell differentiation was analyzed by confocal immunofluorescence
using surface-spread germ cells prepared from control (B) or mutant (D) 9-wk-old testes. In control germ cells, a
combination of anti-HuR and anti-Sycp3 (SCP3) or anti-Sycp3 and anti-γH2AX antibodies reveals the dynamism of HuR
expression during prophase I. In postmeiotic stages, HuR concentrates in round spermatids (RS), but its expression is
lost in elongating spermatids (ES) (B). Inactivation of HuR does not compromise early meiotic events as observed using
a combination of anti-Sycp3 (red) and anti-γH2AX (green) antibodies (D). Cells in meiotic divisions, however, are rarely
observed as revealed by counting cells labeled with a combination of anti-Sycp3 and -γH2AX antibodies: A significant
increase in the number of pachytene spermatocytes and a strong reduction of meiotic cells (diplotene or diakinesis
stage) are observed in mutant cells (E).

successfully completed their meiotic divisions, giving rise to round
spermatids (Figure 2F). These spermatids failed, however, to elongate
at the appropriate stage. Indeed, elongated spermatids appeared
much later in the epithelial cycle and were malformed (Figure 4A). In

adult HuR mutant testes, meiotic divisions were rarely successful, only
occasionally giving rise to round spermatids that failed to begin elon-
gation (Supplemental Figure S2). Therefore spermatogenic defects in
HuR mutant testes occurred in a majority of spermatocytes that did
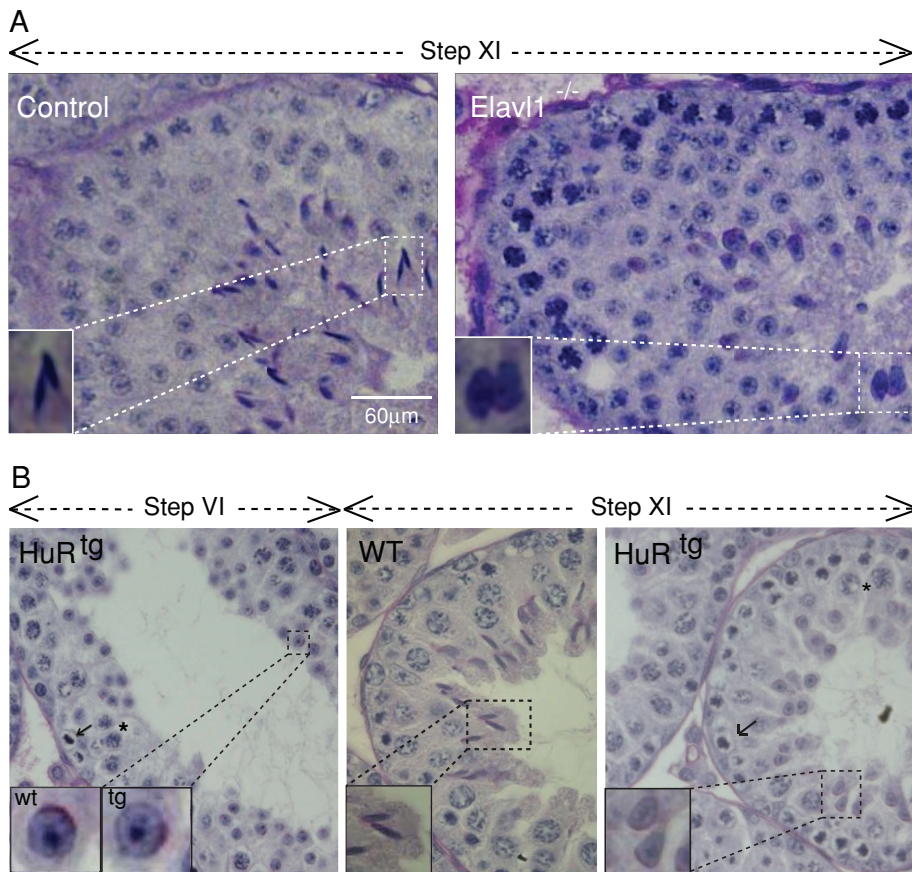
FIGURE 4: Delayed elongation of spermatids in *Elav1⁻/⁻* and HuRᵗᵍ testes. (A and B) Sections from 4-wk-old WT, mutant (Elavl1⁻/⁻) or HuRᵗᵍ testis were stained with periodic acid–Schiff reagent. (A) Pictures were taken at stage XI to illustrate the spermiogenic defects. Whereas numerous elongated spermatids were observed in WT testis, elongation of round spermatids was delayed in HuR mutant testis. Insets show that mutant elongating spermatids are at steps 9–10, but they should be at approximately step 14, as shown in WT. (B) Pictures were taken at step VI and XI of spermatid differentiation to illustrate the spermiogenic defects observed at all stages from step VI. In step VI, as expected, the B mitotic spermatogonia are present (arrow) as well as midpachytene spermatocytes (asterisk). No elongating spermatids are present, however. In addition, the number of round spermatids is reduced, and those present show a developmental delay, as their acrosome is more typical of stage V (zoom in the inset) than stage VI (inset showing WT step 6 spermatid). At step XI, spermatocytes in zygotene (arrow) and diplotene (asterisk) phases of the meiotic prophase are present. Spermatids have initiated elongation, but show delay compared with age-matched WT. They appear much more like step IX (see inset).

ended with a restricted list of genes and focused on *Hsp70-2/Hspa2* not only because the meiotic arrest observed in HuR-deficient germ cells resembles the one described in HSPA2 mutant germ cells (Dix *et al.*, 1996), but also because of increasing evidence for a role of HSPA2 in spermiogenesis (Govin *et al.*, 2006). HSPA2 is a member of the HSP70 family that is expressed exclusively in male germ cells (reviewed in Eddy, 1999). Its depletion induces male but not female infertility, spermatogenic cell development being arrested in prophase of meiosis I at the G2-M-phase (Eddy, 1999).

To test whether *Hspa2* was involved in the phenotype observed in *Elavl1*-mutant germ cells, we studied the expression pattern of HSPA2 protein in *Elavl1⁻/⁻* testes. Immunohistochemical analysis revealed a global decrease compared with control testes (Figure 5, 4 wk). Noticeably, HSPA2 was located primarily in the nuclei of mutant pachytene spermatocytes, whereas in control testes it was abundant both in their nucleus and cytoplasm, as previously reported (Dix *et al.*, 1996). We observed similar results in mutant adult testes (unpublished data). In addition, round spermatids present in some juvenile mutant tubules poorly expressed HSPA2 (Figure 5). Therefore *Hspa2* is misregulated in HuR-deficient germ cells.
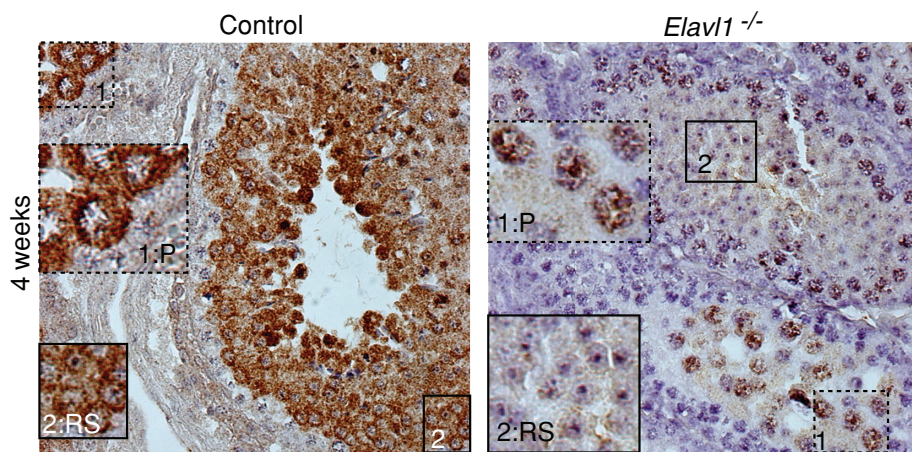
HuR overexpression impairs spermatid differentiation

The scarcity of *Elavl1*-KO males compromises the study of the molecular mechanisms underlying HuR-mediated *Hspa2* misregulation. To overcome this difficulty, we switched to an HuR-overexpression system using transgenic mice that express a Myc-tagged HuR transgene specifically in their germ cells and do not produce fully competent transgenic gametes (Levadoux-Martin *et al.*, 2003). To further characterize the spermatogenic defects, we compared the morphology and histology of WT and transgenic testes at various ages. We observed the first defects at P28, when the transition between round and elongating spermatids takes place (Supplemental Figure S4, D and I). Spermatid differentiation started to be impaired at stage VI: The number of round spermatids was reduced, and their acrosome development was delayed, being typical of stage 5 (Figure 4B). A similar delay of spermatid differentiation was observed in tubules from stage VII to XI. As exemplified in Figure 4B, at stage XI, spermatids from transgenic testes have initiated elongation, but were typical of step 9, whereas in WT testes they were fully elongated. Thus HuR overexpression promotes a delay in the development of round spermatids, a phenotype reminiscent of the one observed in *Elavl1*-deficient spermatids.

Mislocalization of Myc-HuR in transgenic spermatids

We previously reported that HuR subcellular localization was dynamic during WT spermatid differentiation: HuR first accumulates in

not complete meiotic divisions or in the round spermatids derived from the remaining spermatocytes the differentiation of which was blocked before the completion of elongation.

HSPA2 is down-regulated in HuR-deleted germ cells

Because HuR is an RBP known to regulate the expression of numerous but specific genes, we searched for HuR targets the misexpression of which could be responsible for meiotic and postmeiotic defects observed in *Elavl1*-deleted germ cells and carefully analyzed the list of 443 genes recently published the mutations or deletions of which cause reproductive defects (Matzuk and Lamb, 2008). In this list, we selected the genes the mutation of which produces a reproductive phenotype according to the following four criteria: 1) defects are selectively observed in males but not in females; 2) the mutation triggers impairments at late-prophase I or meiotic division stage; 3) the cellular defects are similar to those observed in *Elavl1*-KO testis; and 4) the mutation leads to complete infertility. We thus

Control   Elavl1 −/−

4 weeks

FIGURE 5: Impaired expression of HSPA2 in HuR mutant testes. Immunohistochemical analysis of HSPA2 expression in 4-wk-old control (Elavl1+/−) and Elavl1−/− testes. HSPA2 expression in the KO spermatocytes is mainly nuclear as shown in the enlarged view (1P, for pachytene spermatocyte, right inset), whereas it is both cytoplasmic and nuclear in the WT pachytene spermatocytes (left panel, 1P inset). In addition, HSPA2 is weakly expressed in the round spermatids (2: RS) contained in some mutant tubules (right), whereas it is highly expressed in WT round spermatids (2: RS, left panel).

the CB and then, at steps 4 and 5, exits the CB and associates with polysomes (Nguyen Chi et al., 2009). As the first sign of spermatid differentiation delay observed in HuRtg testis coincided with the step at which HuR exits the CB, we hypothesized that the Myc-HuR transgenic protein could be mislocalized in transgenic spermatids. To test this hypothesis, we subjected adult (P40) testicular extracts to sucrose density gradient fractionation and compared the profile of Myc-HuR sedimentation to that of the endogenous HuR protein in WT extract. Comparison of RNA absorbance profiles between WT and transgenic cytoplasmic extracts showed a slight but reproducible decrease in the amount of polysomes in extracts of transgenic cells (Figure 6A). Western blot analysis revealed a similar distribution of the S6 small ribosomal subunit protein between the two gradients (Figure 6B), indicating that the global translation profile is not altered in HuRtg testes. The endogenous HuR protein distributed throughout the gradient, including the high-molecular-weight fractions that are enriched in polysomes (Figure 6B). By contrast, the Myc-HuR transgenic protein failed to sediment with polysomes but was instead predominantly concentrated in low-molecular-weight fractions (Figure 6, B and C, for quantification). Those fractions include nontranslating mRNA-containing protein complexes (mRNPs) and several components of the CB, such as MVH (Figure 6B), DCP1a (Nguyen Chi et al., 2009), or MIWI and GW182, as described previously (Grivna et al., 2006), suggesting that the transgenic protein might accumulate in the CB or other cytosolic structures that sediment in the RNP fractions. To test this hypothesis, we used immunofluorescence microscopy on seminiferous tubule squash preparations and analyzed endogenous and Myc-HuR localizations during spermatid differentiation. Similarly to the endogenous HuR protein in WT early round spermatids (steps 1–3) (Figure 6D and Nguyen et al., 2009), the transgenic protein accumulated predominantly in the nucleus but was also detected in a perinuclear structure that contains polyadenylated mRNAs and MVH (Figure 6D and Supplemental Figure S5A) and thus corresponds to the CB, as previously reported (Nguyen Chi et al., 2009). In contrast to the WT situation, however, transgenic HuR persisted in the CB of more mature spermatids (83% at steps 4–5) and also accumulated in other cytosolic structures, some of which also contained MVH (Figure 6E). Taken

together, cell fractionation and immunofluorescence experiments show that, in contrast to the WT situation, the transgenic HuR protein is weakly associated to polysomes but accumulates in the CB and other cytosolic structures in transgenic elongating spermatids. Due to its mislocalization, we postulate that the transgenic protein may alter the metabolism of HuR target mRNAs.

**Impaired Hspa2 expression in HuR-overexpressing germ cells**

To test this hypothesis, we analyzed HSPA2 expression in HuRtg testes and observed that HSPA2 expression was indeed decreased upon HuR overexpression, as shown by Western blot analysis of whole-cell extracts (Figure 7A). Although reproducible, the decrease was moderate, suggesting that the defect might take place in a restricted population of germ cells. Analysis at the cellular level using IHC confirmed this hypothesis, showing a particularly strong reduction of HSPA2 in elongating spermatids in adult testes (Figure 7B). The decrease at the protein level was not correlated with a decreased level of Hspa2 mRNA, as similar levels of Hspa2 mRNA were found in WT and transgenic testes both by quantitative RT-PCR (qRT-PCR) and microarray experiments (Figure 7C and unpublished data), but was due to its decreased translation. Indeed, analysis of Hspa2 mRNA relative abundance in the RNP and polysome fractions of the sucrose density gradients described earlier in this article revealed an increased amount of Hspa2 mRNA in RNP fractions and a reduced (≈15%) association with polysomes in transgenic testicular extracts (Figure 7D). By contrast, the relative abundance in the RNP and polysome fractions of two control mRNAs that do not bind HuR, PGK2 and the longest GCNF transcript (Yang et al., 2003), was similar in transgenic and control extracts (Supplemental Figure S6).

These data suggested that HuR binds Hspa2 mRNA and regulates its expression. To test this hypothesis, we performed a RNA-IP assay using cytoplasmic testicular extracts from P17 or 6-wk-old WT males that did not yet contain haploid cells or were enriched in spermatids, respectively. We observed that Hspa2 mRNA was specifically retained by anti-HuR antibody in both types of cytoplasmic extracts. Interestingly, the enrichment of the Hspa2 mRNA in HuR IP was more important (≈20-fold) in adult than in P17 samples (Figure 7E and Supplemental Figure S7B), whereas HuR level was unchanged (Nguyen Chi et al., 2009), suggesting that HuR affinity for Hspa2 mRNAs increased between meiotic and postmeiotic stages. Similarly, Hspa2 mRNA was specifically retained by anti-Myc antibody in transgenic extracts (Figure 7E). All together, these results show that HuR and HuR transgenic proteins bind Hspa2 mRNA and strongly suggest that HuR up-regulates Hspa2 mRNA translation during spermatogenesis in a specific and direct manner.

DISCUSSION

Spermatogenesis is a complex process that relies on extensive regulation of mRNA storage and translation. In this study, we have investigated the role of the RBP HuR in mammalian spermatogenesis by using both germ cell–specific loss- and gain-of-function strategies. We have provided evidence that HuR is essential for male germ cell differentiation. In addition, at the
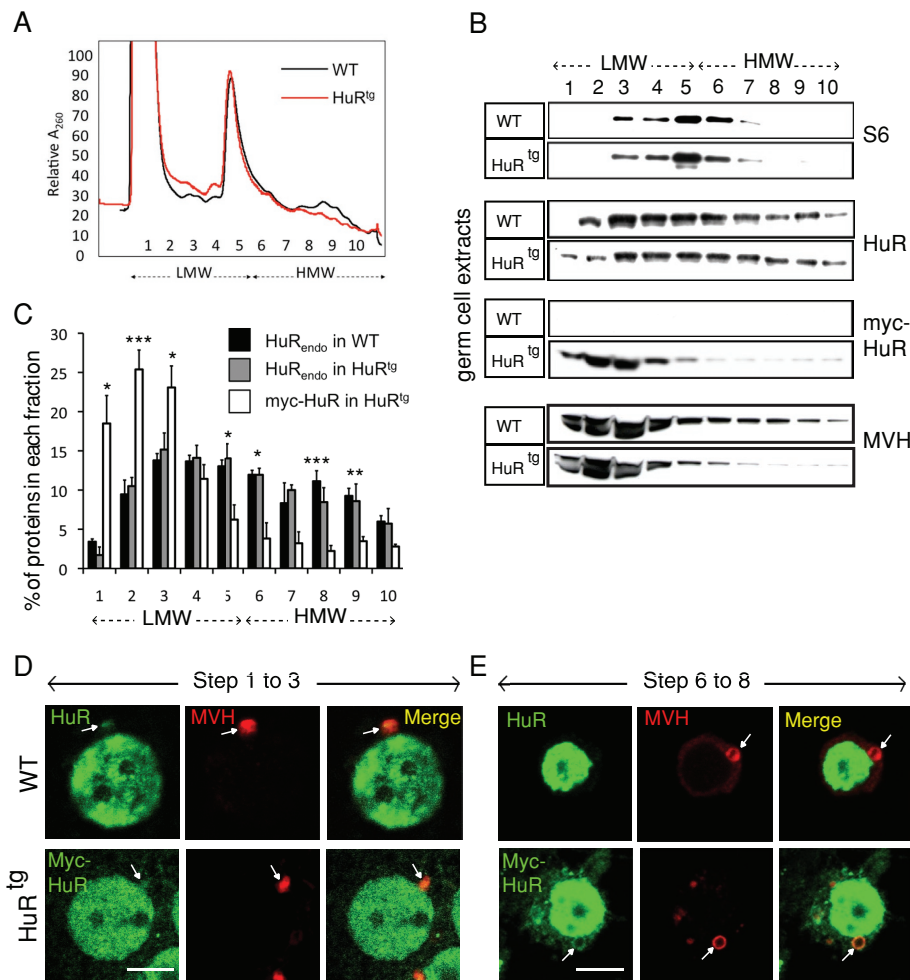
FIGURE 6: HuR exit from the CB is compromised in HuR^tg spermatids. (A–C) Germ cell cytoplasmic extracts from a pool of 10 P40 WT or transgenic (HuR^tg) testes were fractionated on 15–50% sucrose density gradients. RNA absorbance profiles at 260 nm are shown. Low-molecular-weight (LMW) fractions (fractions 1–5) contain RNP complexes, components of the CB and ribosome subunits. High-molecular-weight (HMW) fractions (6–10) include polysomes (A). Proteins were extracted from each fraction and analyzed by Western blot using anti-S6, anti-endogenous HuR, anti-Myc, or anti-MVH antibodies (B). The distribution of endogenous HuR (HuR) in both WT and transgenic (HuR^tg) extracts is different from that of the transgenic HuR protein (myc-HuR) as revealed by quantification of three independent gradients. Their level of expression in a given fraction is given as the percentage of the level found in all fractions (C). *p < 0.05, **p < 0.01, and ***p < 0.005. (D and E) Round spermatids at the indicated steps of differentiation were prepared from tubule squashes of WT and HuR^tg testes. Cells were doubly stained with anti-HuR (or anti-Myc that specifically recognizes the transgenic protein) (green) and anti-MVH (red) antibodies. In WT, both MVH and HuR localize within the CB of early (steps 1–3) round spermatids (arrow), and HuR exits the CB at further steps of differentiation. In transgenic spermatids, HuR stays in the CB of more mature spermatids (steps 6–8) (arrow).

end of prophase I stages, does not affect the normal progression of meiotic prophase, indicating that HuR most probably does not control expression of genes involved in chromosome pairing, double-strand breaks, and/or DNA repair the mutations of which provoke a halt during the meiotic prophase I (Kuznetsov et al., 2007). HuR mutant germ cells, however, fail to progress further on. Spermatocytes die during meiotic divisions, and spermatids are lacking in nearly all tubules of adult testes, showing that HuR is required for the completion of meiosis. In contrast, HuR^tg spermatocytes divide correctly, most probably because HuR^tg is not highly overexpressed in these cells. Indeed, we estimated that the amount of *HuR* mRNA (endogenous plus transgenic) in transgenic spermatocytes was only fivefold higher than in WT spermatocytes, whereas transgenic postmeiotic cells that exhibit differentiation defects (see below) express nearly 20-fold more HuR than the WT ones (Supplemental Figure S3).

HuR is required for spermiogenesis completion

In adults, despite a nearly complete failure of germ cells to progress through meiotic divisions, some spermatocytes manage to divide and give rise to round spermatids that fail to elongate. In juvenile mutant testes, some tubules contain round spermatids, but their differentiation is delayed, leading to an absence of elongated spermatids or malformed ones. A similar differentiation delay is observed in HuR^tg spermatids. The majority of HuR^tg males, however, are fertile most probably because WT haploid cells that do not accumulate the HuR transgenic protein at a detrimental level normally differentiate into sperm (Levadoux-Martin et al., 2003). Thus beside its role during meiotic phase, HuR is also required for spermatid differentiation, during which it may play a role in chromatin condensation and/or cell elongation, two major events of spermiogenesis.

HuR controls Hspa2 mRNA translation

As mentioned earlier in this article, in the list

molecular level, we have identified Hspa2/Hsp70-2, an essential regulator of spermatogenesis, as a direct downstream target of HuR.

HuR is a key regulator of meiotic division in males

Specific deletion of HuR in germ cells leads to male sterility, associated with dramatically reduced testis size, spermatogenic defects, and absence of spermatozoa in the epididymides. In sharp contrast with hematopoietic and intestinal systems (Ghosh et al., 2009), HuR is not essential for progenitor germ cell survival in gametogenesis because it starts to accumulate in midpachytene spermatocytes. Therefore its deletion at earlier stages, from the leptotene to the

of genes the mutations or deletions of which cause reproductive defects (Matzuk and Lamb, 2008), we selected *Hspa2/Hsp70-2* because 1) absence of HSPA2 leads to complete male sterility and meiotic disorders that resemble those observed in HuR-deficient germ cells (Dix et al., 1996) and 2) *Hspa2/Hsp70-2* may represent a target of HuR not only in meiosis but also in spermiogenesis, during which HSPA2 has been proposed to play a decisive role in genome-wide reorganization occurring during postmeiotic stages (Quenet et al., 2009). We have observed that HSPA2 expression is down-regulated in HuR-deleted and -overexpressing haploid germ cells and that endogenous and transgenic HuR proteins bind *Hspa2* mRNA in germ cells. Further studies will be needed to know whether
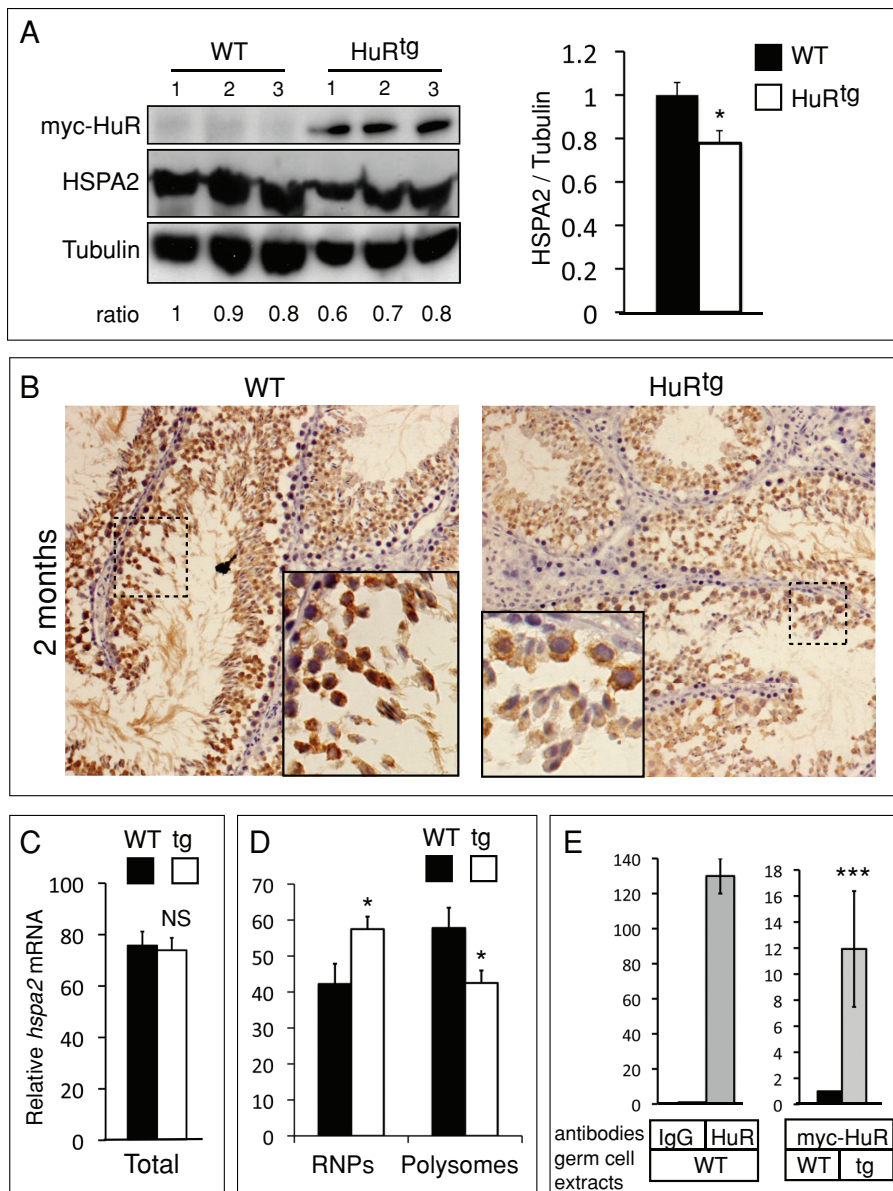
FIGURE 7: Impaired expression of HSPA2 in HuR[tg] testes. (A) Western blot analysis of Myc-HuR transgene and HSPA2 expression in WT (1–3) and transgenic (4–6) testes. Quantification of HSPA2 signals and normalization to tubulin signals reveals a slight but reproducible and significant decrease of HSPA2 expression in transgenic tubules (*p < 0.05). (B) Immunohistochemical analysis of HSPA2 expression in 2-mo-old WT and HuR[tg] testes. HSPA2 expression is particularly decreased in the haploid cells of transgenic tubules. (C) Gene expression profiles from P28 WT and HuR[tg] testes were analyzed using the Affymetrix microarrays approach (unpublished data). The relative *Hspa2* mRNA expression after normalization indicates no significant difference between WT and transgenic testes (p = 0.66). (D) qRT-PCR detection of *Hspa2* mRNA in mRNP and polysomal fractions from control and HuR[tg] testes. Data are derived from measurements in pooled fractions (1–5, mRNPs, 6–10, polysomes) normalized to 18S rRNA and presented as percentages of total cytoplasmic *Hspa2* mRNA in each condition. The values were obtained after analysis of three independent sucrose gradient experiments, each one using a pool of 6–10 testes from P40 WT or HuR[tg] males (p < 0.05). (E) HuR endogenous and transgenic proteins bind *Hspa2* mRNA. Cytoplasmic extracts from testes of 6-wk-old WT males were prepared and immunoprecipitated using anti-HuR antibody. Control immunoglobulin was used in parallel (left panel). Similarly, cytoplasmic germ cell extracts were prepared from a pool of P28 WT or HuR[tg] testes (right panel). RNA-IP was performed using anti-Myc antibody (9E10) using the same amount of WT and HuR[tg] protein extracts. RNAs were extracted. The amount of *Hspa2* mRNA retained in the immunoprecipitates was analyzed by qRT-PCR. Amplification of contaminating traces of 18S rRNA was performed as an internal control that serves for normalization. Three independent experiments using different pools of WT and HuR[tg] germ cells were performed. SEMs are shown; ***p < 0.005.

HuR directly binds *Hspa2* mRNA and to determine the sequences involved. The analysis of the *Hspa2* 3′UTR, however, revealed two AUUUA pentamers and four U-rich sequences that are conserved in mammals (Supplemental Figure S7A), and represent potential binding sites for HuR (Mukherjee *et al.*, 2009). The association of *Hspa2* mRNA with translating ribosomes was decreased in HuR[tg] germ cells, leading to a reduced level of HSPA2 protein, particularly in elongating spermatids. Decreased *Hspa2* mRNA translation was correlated with a strong association of Myc-HuR with mRNPs and a concomitant failure to accumulate in polysomes, a behavior that sharply contrasts with HuR in a WT context, suggesting that the transgenic protein behaves as a dominant- negative form of HuR. Our data led us to propose the following model (Figure 8): In WT spermatids, HuR binds to *Hspa2* mRNA and allows HSPA2 synthesis during spermatid differentiation (Eddy, 1999). By contrast in transgenic spermatids, the transgenic protein binds to *Hspa2* mRNAs but fails to associate with translating polysomes, preventing *Hspa2* translation. Similarly, the absence of HuR results in *Hspa2* translation inhibition in *Elavl1*^{−/−} spermatids. The decrease of HSPA2 expression in both situations might be responsible for spermatid development arrest. In addition, HSPA2 expression is down-regulated in HuR-deficient spermatocytes, and HuR binds *Hspa2* mRNA at this stage. Therefore we propose that HuR also controls *Hspa2* mRNA translation during meiosis. We have noticed a decrease, however, in the cytoplasmic level of HSPA2 both in adult and juvenile spermatocytes, suggesting that additional HuR-mediated regulatory mechanisms, such as nucleocytoplasmic trafficking or stability of HSPA2 protein, might be involved.

Although related, there are nevertheless some differences between the phenotypes of HSPA2- and HuR-deficient mouse testes. Globally, HuR deficiency is slightly less severe than HSPA2 deficiency, possibly because other members of the Hu family might compensate for HuR absence. Besides *Hspa2*, the list of candidate genes contained four other genes that retained our attention: *cyclin A1* (Liu *et al.*, 1998; Nickerson *et al.*, 2007), *Gal3st1* (Honke *et al.*, 2002), *Dmrt7* (Kawamata and Nishimori, 2006), and *Parp2* (Quenet *et al.*, 2009) because they encode mRNAs containing putative HuR binding sites. Should their binding to HuR be demonstrated in germ cells, expression of those genes might be modified together with HSPA2 in HuR-deficient germ cells, contributing to the observed phenotype. Clearly
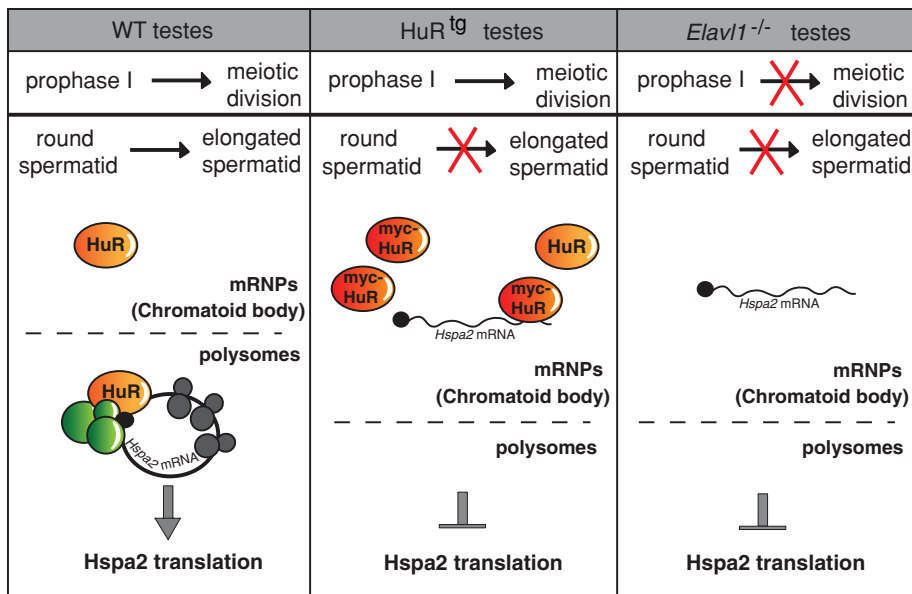
FIGURE 8: A model for the role of HuR in the translational control of its *Hspa 2* target mRNA in WT or HuR-overexpressing or -deficient germ cells. Effects of manipulating HuR level of expression on spermatogenesis progression are shown. Absence of HuR leads to meiotic defects whereas mild HuR overexpression does not alter early spermatogenesis. In spermiogenesis, both HuR deletion and strong overexpression result in spermatid differentiation arrest. The cytoplasm of spermatids has been schematically divided into two compartments, mRNPs (including the CB) corresponding to untranslating mRNAs, and polysomes, where the translation is active. In WT spermatids, HuR binds to *Hspa2* mRNAs in mRNPs and polysomes, ensuring their regulated translation. In HuR[tg] spermatids, HuR overexpression results in the nearly complete loss of HuR association to polysomes, leading to translational inhibition of *Hspa2* mRNA, a situation similar to the one observed in *Elav1^{−/−}* germ cells.

further studies are required to characterize all the mRNAs the translation of which is impaired following HuR deletion and to reinforce the conclusions we have drawn from the limited number of animals. A first step toward this challenging goal relies on Cre-expressing lines that should fulfill two requirements: 1) the recombination should be fully efficient in all germ cells to avoid HuR trafficking through cytoplasmic bridges from cells in which recombination has not taken place to *Elavl1^{−}* cells; and 2) the Cre recombinase should not be active during embryonic development because HuR activity is essential for life (Ghosh *et al.*, 2009; Katsanou *et al.*, 2009).

To conclude, we have shown that manipulating HuR expression results in dramatic spermatogenic defects leading to male infertility. Our study provides the first genetic evidence that HuR is crucial for spermatogenesis and highlights the key role of RBPs in controlling this process.

MATERIALS AND METHODS
Production of HuR-deleted or -overexpressing mice
Mice were maintained in accordance with institutional guidelines (French National Center for Scientific Research; CNRS). Their use followed the French laws and was in accordance with the European Directive (86/609/EEC). The transgenic mice overexpressing HuR were produced and genotyped as described previously (Gouble *et al.*, 2002). The strategy to generate and genotype *Elavl1^{fl/fl}*, *Elavl1^{fl/−}*, or *Elavl1^{+/−}* mice has been described (Katsanou *et al.*, 2009). The different strains expressing the Cre recombinase were first mated with *Elavl1^{+/−}* mice to produce *Elavl1^{+/−}*. Cre males were then crossed with *Elavl1^{fl/fl}* following the scheme described in Figure 1A to obtain HuR-deleted germ cells.

Collection of tissues, purification of spermatogenic cells, tubule squashes, in situ hybridization on tubule squashes, and sucrose density fractionation were performed as described previously (Nguyen Chi *et al.*, 2009) with the following antibodies: rabbit anti-SYCP3 and anti-γH2AX (Novus Biologicals, Littleton, CO), anti-MVH (Abcam, Cambridge, MA), anti-HuR (19F12; Clonegene, Hartford, CT), Myc (9E10; Santa Cruz Biotechnology, Santa Cruz, CA). Anti-HSPA2 antibody was provided by E.M. Eddy (NIEHS, NIH). Nuclei were labeled with TO-PRO3 or DAPI (Molecular Probes, Eugene, OR). Polyadenylated mRNAs were detected by in situ hybridization on tubule squash preparations, using a biotinylated DNA oligo(dT) probe, as described (Nguyen Chi *et al.*, 2009). Images were obtained with a Leica SP2 or SP5 confocal microscope equipped with helium-neon lasers and appropriate filter combinations.

Histological and IHC analyses. Testes and epididymides were stored in aqueous Bouin's solution for 48 h and in ethanol 70% before embedding in paraffin wax. Sections (5 μm thick) were stained with either hematoxylin and eosin (H&E) or by the periodic acid–Schiff technique. Analysis of HSPA2 on testis sections was performed by IHC as described (Dix *et al.*, 1997). Sections were counterstained with hematoxylin.

RNA-IP experiment. Briefly, tunica albuginea was removed from 10 to 20 P17 testes that were subsequently minced in phosphate-buffered saline. Cells were collected without debris after sedimentation (5 min, 4°C) and centrifuged for 5 min at 4°C and 1500 rpm. Germ cell suspension preparation for P28 old testes and the IP experiment were performed as described previously (Nguyen Chi *et al.*, 2009). Total RNA from cytoplasmic extracts or immunoprecipitated materials was extracted with TRIzol reagent, reverse transcribed, and qRT-PCR amplified using a Bio-Rad (MyiQ; Hercules, CA) instrument and Hspa2 primers (forward: CAG-TCA-GGA-TGT-CTG-CCC-GCG; reverse: GTC-GCC-GAT-GAG-ACG-CTC-GG) and 18S rRNA primers (forward: GTA-ACC-CGT-TGA-ACC-CCA-TT; reverse: CCA-TCC-AAT-CGG-TAG-TAG-CG) to normalize RNA levels.

Statistical analyses. mRNA was extracted from the testes of three P28 WT and three HuR[tg] mice. Transcript expression analysis was performed using Affymetrix microarrays. *Hspa2* mRNA expression was normalized using the GC-RMA algorithm. Mean and standard errors of the mean were determined with at least three independent experiments. Values of p were calculated using the two-tailed unpaired *t* test.

REFERENCES

Bevilacqua A, Ceriani MC, Capaccioli S, Nicolin A (2003). Post-transcriptional regulation of gene expression by degradation of messenger RNAs. J Cell Physiol 195, 356–372.

de Boer J et al. (2003). Transgenic mice with hematopoietic and lymphoid specific expression of Cre. Eur J Immunol 33, 314–325.

Deng W, Lin H (2002). miwi, a murine homolog of piwi, encodes a cytoplasmic protein essential for spermatogenesis. Dev Cell 2, 819–830.

Dix DJ, Allen JW, Collins BW, Mori C, Nakamura N, Poorman-Allen P, Goulding EH, Eddy EM (1996). Targeted gene disruption of Hsp70-2 results in failed meiosis, germ cell apoptosis, and male infertility. Proc Natl Acad Sci USA 93, 3264–3268.

Dix DJ, Allen JW, Collins BW, Poorman-Allen P, Mori C, Blizard DR, Brown PR, Goulding EH, Strong BD, Eddy EM (1997). HSP70-2 is required for desynapsis of synaptonemal complexes during meiotic prophase in juvenile and adult mouse spermatocytes. Development 124, 4595–4603.

Eddy EM (1999). Role of heat shock protein HSP70-2 in spermatogenesis. Rev Reprod 4, 23–30.

Galban S et al. (2008). RNA-binding proteins HuR and PTB promote the translation of hypoxia-inducible factor 1alpha. Mol Cell Biol 28, 93–107.

Gallardo T, Shirley L, John GB, Castrillon DH (2007). Generation of a germ cell-specific mouse transgenic Cre line, Vasa-Cre. Genesis 45, 413–417.

Ghosh M, Aguila HL, Michaud J, Ai Y, Wu MT, Hemmes A, Ristimaki A, Guo C, Furneaux H, Hla T (2009). Essential role of the RNA-binding protein HuR in progenitor cell survival in mice. J Clin Invest 119, 3530–3543.

Gouble A, Grazide S, Meggetto F, Mercier P, Delsol G, Morello D (2002). A new player in oncogenesis: AUF1/hnRNPD overexpression leads to tumorigenesis in transgenic mice. Cancer Res 62, 1489–1495.

Govin J, Caron C, Escoffier E, Ferro M, Kuhn L, Rousseaux S, Eddy EM, Garin J, Khochbin S (2006). Post-meiotic shifts in HSPA2/HSP70.2 chaperone activity during mouse spermatogenesis. J Biol Chem 281, 37888–37892.

Grivna ST, Pyhtila B, Lin H (2006). MIWI associates with translational machinery and PIWI-interacting RNAs (piRNAs) in regulating spermatogenesis. Proc Natl Acad Sci USA 103, 13415–13420.

Honke K et al. (2002). Paranodal junction formation and spermatogenesis require sulfoglycolipids. Proc Natl Acad Sci USA 99, 4227–4232.

Iguchi N, Tobias JW, Hecht NB (2006). Expression profiling reveals meiotic male germ cell mRNAs that are translationally up- and down-regulated. Proc Natl Acad Sci USA 103, 7712–7717.

Katsanou V, Milatos S, Yiakouvaki A, Sgantzis N, Kotsoni A, Alexiou M, Harokopos V, Aidinis V, Hemberger M, Kontoyiannis DL (2009). The RNA-binding protein Elavl1/HuR is essential for placental branching morphogenesis and embryonic development. Mol Cell Biol 29, 2762–2776.

Katsanou V, Papadaki O, Milatos S, Blackshear PJ, Anderson P, Kollias G, Kontoyiannis DL (2005). HuR as a negative posttranscriptional modulator in inflammation. Mol Cell 19, 777–789.

Kawamata M, Nishimori K (2006). Mice deficient in Dmrt7 show infertility with spermatogenic arrest at pachytene stage. FEBS Lett 580, 6442–6446.

Kimmins S, Sassone-Corsi P (2005). Chromatin remodelling and epigenetic features of germ cells. Nature 434, 583–589.

Kotaja N, Bhattacharyya SN, Jaskiewicz L, Kimmins S, Parvinen M, Filipowicz W, Sassone-Corsi P (2006). The chromatoid body of male germ cells: similarity with processing bodies and presence of Dicer and microRNA pathway components. Proc Natl Acad Sci USA 103, 2647–2652.

Kotaja N, Kimmins S, Brancorsini S, Hentsch D, Vonesch JL, Davidson I, Parvinen M, Sassone-Corsi P (2004). Preparation, isolation and characterization of stage-specific spermatogenic cells for cellular and molecular analysis. Nat Methods 1, 249–254.

Kress C, Gautier-Courteille C, Osborne HB, Babinet C, Paillard L (2007). Inactivation of CUG-BP1/CELF1 causes growth, viability, and spermatogenesis defects in mice. Mol Cell Biol 27, 1146–1157.

Kuznetsov S et al. (2007). RAD51C deficiency in mice results in early prophase I arrest in males and sister chromatid separation at metaphase II in females. J Cell Biol 176, 581–592.

Lammers JH, Offenberg HH, van Aalderen M, Vink AC, Dietrich AJ, Heyting C (1994). The gene encoding a major component of the lateral elements of synaptonemal complexes of the rat is related to X-linked lymphocyte-regulated genes. Mol Cell Biol 14, 1137–1146.

Levadoux-Martin M, Gouble A, Jegou B, Vallet-Erdtmann V, Auriol J, Mercier P, Morello D (2003). Impaired gametogenesis in mice that overexpress the RNA-binding protein HuR. EMBO Rep 4, 394–399.

Liu D, Matzuk MM, Sung WK, Guo Q, Wang P, Wolgemuth DJ (1998). Cyclin A1 is required for meiosis in the male mouse. Nat Genet 20, 377–380.

Lopez de Silanes I, Zhan M, Lal A, Yang X, Gorospe M (2004). Identification of a target RNA motif for RNA-binding protein HuR. Proc Natl Acad Sci USA 101, 2987–2992.

Ma WJ, Cheng S, Campbell C, Wright A, Furneaux H (1996). Cloning and characterization of HuR, a ubiquitously expressed Elav-like protein. J Biol Chem 5, 8144–8151.

Mahadevaiah SK, Turner JM, Baudat F, Rogakou EP, de Boer P, Blanco-Rodriguez J, Jasin M, Keeney S, Bonner WM, Burgoyne PS (2001). Recombinational DNA double-strand breaks in mice precede synapsis. Nat Genet 27, 271–276.

Matzuk MM, Lamb DJ (2008). The biology of infertility: research advances and clinical challenges. Nat Med 14, 1197–1213.

Mukherjee N, Lager PJ, Friedersdorf MB, Thompson MA, Keene JD (2009). Coordinated posttranscriptional mRNA population dynamics during T-cell activation. Mol Syst Biol 5, 288.

Myer VE, Fan XC, Steitz JA (1997). Identification of HuR as a protein implicated in AUUUA-mediated mRNA decay. EMBO J 16, 2130–2139.

Nguyen Chi M, Chalmel F, Agius E, Vanzo N, Khabar KS, Jegou B, Morello D (2009). Temporally regulated traffic of HuR and its associated ARE-containing mRNAs from the chromatoid body to polysomes during mouse spermatogenesis. PLoS One 4, e4900.

Nickerson HD, Joshi A, Wolgemuth DJ (2007). Cyclin A1-deficient mice lack histone H3 serine 10 phosphorylation and exhibit altered aurora B dynamics in late prophase of male meiosis. Dev Biol 306, 725–735.

Parvinen M (2005). The chromatoid body in spermatogenesis. Int J Androl 28, 189–201.

Quenet D, Mark M, Govin J, van Dorsselear A, Schreiber V, Khochbin S, Dantzer F (2009). Parp2 is required for the differentiation of post-meiotic germ cells: identification of a spermatid-specific complex containing Parp1, Parp2, TP2 and HSPA2. Exp Cell Res 315, 2824–2834.

Steger K (1999). Transcriptional and translational regulation of gene expression in haploid spermatids. Anat Embryol (Berl) 199, 471–487.

Steger K (2001). Haploid spermatids exhibit translationally repressed mRNAs. Anat Embryol (Berl) 203, 323–334.

Tsai-Morris CH, Sheng Y, Lee E, Lei KJ, Dufau ML (2004). Gonadotropin-regulated testicular RNA helicase (GRTH/Ddx25) is essential for spermatid development and completion of spermatogenesis. Proc Natl Acad Sci USA 101, 6373–6378.

Turner JM, Burgoyne PS, Singh PB (2001). M31 and macroH2A1.2 colocalise at the pseudoautosomal region during mouse meiosis. J Cell Sci 114, 3367–3375.

Vidal F, Sage J, Cuzin F, Rassoulzadegan M (1998). Cre expression in primary spermatocytes: a tool for genetic engineering of the germ line. Mol Reprod Dev 51, 274–280.

Yang G, Zhang YL, Buchold GM, Jetten AM, O'Brien DA (2003). Analysis of germ cell nuclear factor transcripts and protein expression during spermatogenesis. Biol Reprod 68, 1620–1630.

Yang J, Medvedev S, Yu J, Tang LC, Agno JE, Matzuk MM, Schultz RM, Hecht NB (2005). Absence of the DNA-/RNA-binding protein MSY2 results in male and female infertility. Proc Natl Acad Sci USA 102, 5755–5760.